RSC Advances

ROYAL SOCIETY OF CHEMISTRY

www.rsc.org/advances

Sanguinarine, a promising anticancer therapeutic: Photochemical and nucleic acid binding properties

Gopinatha Suresh Kumar[*] and Soumitra Hazra

Biophysical Chemistry Laboratory, Chemistry Division

CSIR-Indian Institute of Chemical Biology

Kolkata 700 032, India

Address for Correspondence:

Dr. G. Suresh Kumar

Senior Principal Scientist

Biophysical Chemistry Laboratory

CSIR-Indian Institute of Chemical Biology

4, Raja S. C. Mullick Road, Jadavpur

Kolkata 700032, INDIA

Phone: +91 33 2472 4049 /2499 5723

Fax: +91 33 2473 0284 / 5197

e-mail: gskumar@iicb.res.in/gskumar@csiriicb.in

Sanguinarine is a benzophenanthridine plant alkaloid with remarkable therapeutic utility. It undergoes photochemical changes and also forms strong complexes with nucleic acids, the latter being considered to be one of the important aspects for its therapeutic utility, particularly the anticancer activity. This review highlights the photochemical aspects of sanguinarine and the binding properties to various structural forms of DNA and RNA as reported from a variety of physicochemical and calorimetric studies. These may serve as guiding factors for the development of sanguinarine as a therapeutic agent.

1. Introduction

Sanguinarine (Fig. 1) is one of the most important members of the relatively small group of quaternary benzo[c]phenanthridine alkaloids (QBAs). This alkaloid is found in a number of medicinal plant families like *Papaveraceae, Fumariaceae, Rutaceae, Sanguinaria canadensis (blood root), Poppy fumaria, Bocconia frutescens, Chelidonium majus, Macleya cordata*. Sanguinarine exhibits diverse biological effects. It was initially shown that sanguinarine possesses anti-bacterial and anti inflammatory properties.[1,2] The antimicrobial activity of sanguinarine is well known.[2,3] The antimicrobial and anti inflammatory activities merited its use in dental hygiene products.[4] The principal pharmacological application of sanguinarine so far has been in oral care products for its antiplaque and antigingivitis activities. Its anti-plaque action is by inhibition of bacterial adherence to newly formed pellicle.[2]

Sanguinarine exhibited the highest cytotoxicity among benzophenanthridine alkaloids as reported by Slaninova et al.[5] Studies have shown that sanguinarine induces apoptosis in a variety of cancer cells via cell cycle arrest,[6] caspase activation,[7] depletion of cellular GSH,[8] and subsequent caspase activation,[9] modulation of the family of Bcl-2,[10] down-regulation of ERKs,[11] and up-regulation of DR-5[12] etc. Sanguinarine causes cell cycle blockade and apoptosis of human prostate carcinoma cells via modulation of cyclin kinase inhibitor-cyclin-cyclin-dependent kinase machinery.[6] Sanguinarine also arrests LNCaP and DU145 cells in G1 phase. Sanguinarine has been shown to down regulate the IAP family proteins cIAP1, cIAP2, and XIAP in human primary effusion lymphoma

cell lines.[13] Suppression of BLBC growth by sanguinarine was correlated with the p27 and down regulation of cyclin D1, and with the inhibition of STAT3 activation.[14] Interestingly, reports suggested that sanguinarine does not exert an apoptotic affect on normal cells and therefore can be developed as an effective anticancer drug.[15]

Sanguinarine is a potent inhibitor for Na-K-dependent ATPase, cholinesterase,[16,17] NF-kB and mitogen-activated protein kinase phosphatase-1.[18] Sanguinarine binds and perturbs the secondary structure of tubulin.[19] In fact plants containing sanguinarine have been used as Chinese medicines and folk medicines for treatment of human cancer. However, FDA so far has not yet approved any products containing sanguinarine for the treatment of cancer. The anticancer and other biological activities of sanguinarine have been reviewed in many articles.[20-25]

Sanguinarine exhibits strong photochemical activities and is a strong DNA and RNA interacting molecule. Its nucleic acid binding properties have often been linked to its strong anticancer activities. This review summarizes the *in vitro* studies focused on the nucleic acid binding properties of sanguinarine that may correlate to its potential medicinal efficacy.

2. Chemistry of synthesis

Sanguinarine (SG) is 13-methyl-[1.3]-benzodioxolo[5,6-c]-1,3-dioxolo[4,5-*i*] phenanthradin-13-ium (Fig. 1). The biosynthetic pathway involves the condensation of two L-Tyr derivatives to yield the central precursor (*S*)-norcoclaurine.[26] Specific *O*-, and *N*-methyl transferases convert (*S*)-norcoclaurine to (*S*)-*N*-methylcoclaurine.[27] The

P450-dependent monooxygenase (*S*)-*N*-methylcoclaurine-3′-hydroxylase (CYP80B1) catalyzes the 3′-hydroxylation of (*S*)-*N*-methylcoclaurine.[28] The subsequent 4′-*O*-methylation of (*S*)-3′-hydroxy-*N*-methylcoclaurine yields (*S*)-reticuline.[27] The berberine bridge enzyme (BBE) catalyzes the conversion of (*S*)-reticuline to (*S*)-scoulerine, the first committed step in the sanguinarine biosynthetic pathway.[29] Protopine is an important intermediate in its synthesis. Hydroxylation of protopine with NADPH as a reduction cofactor and molecular oxygen results in the formation of dihydrosanguinarine (DHSG). This reaction is catalyzed by a microsomal cytochrome P450-linked monooxygenase. The enzyme dihydrobenzophenanthridine then converts DHSG to sanguinarine.[30] Sanguinarine and DHSG have also been synthesized from coptisine.[31]

3. Physical properties

Sanguinarine is an orange red colored crystalline compound. It occurs generally as chloride and some time as sulfate salts. It is slightly soluble in water and highly soluble in organic solvents. The physicochemical properties of sanguinarine are presented in Table 1.

4. Acid-base equilibrium of sanguinarine

One of the most important properties of the QBAs is their ability to exist in two different structures in aqueous solutions depending on the pH. Sanguinarine can exist as a quaternary cation (the iminium form) and 6-hydroxydihydroderivative (pseudo base) or alkanolamine form (Scheme 1). Since the carbon atom at the 6 position of sanguinarine has low electron density, it is easily susceptible to nucleophilic addition of

OH ions. So in alkaline aqueous solutions, OH$^-$ binds to the quaternary ammonium form to afford the 6-hydroxyderivative. The reversible, pH dependent equilibrium between the charged iminium and the neutral alkanolamine forms in aqueous solution may be described by the equation $SG^+ + OH^-$ $SGOH$.[20] These two forms have characteristic absorbance and fluorescence spectra which are shown in Fig. 2. The equilibrium between the water-soluble cationic form and the less soluble neutral alkanolamine is characterized by a pKa of about 8.06.[32,33] Thus, both forms of the alkaloid are present in solution at physiological pH and may engage themselves in interactions with biological systems. While the iminium form is unsaturated and completely planar, the alkanolamine form has a buckled structure and non-planar. The non-polar (lipophilic) pseudo base can penetrate the cell membrane increasing its cellular availability. Once inside the cell it may be converted partially to the iminium form depending on the pH and other factors.

5. Photochemical and toxic properties

Sanguinarine is a brightly colored molecule with strong absorption bands in the UV-vis region and fluorescence emission due to the conjugated and highly aromatic character of its chromophore. The molecule is, therefore, sensitive to light and have adverse phototoxic reactions if exposed to sunlight. The alkanolamine form of sanguinarine has been revealed to undergo photochemical changes producing oxysanguianrine in the presence of oxygen (Scheme 2).[34] The fluorescence signal of sanguinarine at 418 nm in aqueous buffer at pH 11 is unstable due to this oxidative photoreaction. The

photooxidation of sanguinarine was also studied in oxygenated alkaline methanol solutions and it was found that the presence of Rose Bengal as photosensitizer significantly accelerated the process suggesting the importance of singlet molecular oxygen in the reaction mechanism. The sensitized oxidation of the sanguinarine alkanolamine form was suggested to follow the sequence involving the radical cation SG-OH· $^+$, the radical SG-O· and two molecules of O_2 ($^1\Delta g$). It was also found that the uncharged pseudobase form is oxidized much more easily than the charged cation.[35]

The toxicity of sanguinarine has also been suggested to be due to its DNA intercalation, inhibition of ion pumps and several SH-dependent proteins, and interaction with cytoskeletal components.[36,37] Sanguinarine can kill animal cells through its action on the Na^+-K^+-ATPase transmembrane protein. Epidemic dropsy is a form of edema of extremities that results from ingesting argemone oil containing sanguinarine. It has been found that application of sanguinarine to skin may destroy the tissues. Phototoxic effect of sanguinarine against mosquito larvae has also been reported.[38] Time-resolved emission studies indicated that sanguinarine produces a significant amount of singlet oxygen.[39] The singlet oxygen production by sanguinarine has been observed by Maiti[40] et al. also. On the other hand, the toxicity of catalase-deficient strains of *Escherichia coli* has been reported and the phototoxic action has been suggested to involve production of H_2O_2.[41]

Reactive oxygen species (ROS) such as superoxide anions (O_2^-) or hydrogen peroxide (H_2O_2) have also been found to be generated in sanguinarine-treated cells.[42-45] Recent

studies have also suggested that sanguinarine inhibited the growth cancer cells and induced their apoptosis through the generation of free radicals.[46]

6. 1. DNA binding properties of sanguinarine

Sanguinarine exhibits various pharmacological effects and is a potential lead compound in cancer chemotherapy inducing apoptosis in a variety of cancer cells through various mechanisms. One of the most important properties of sanguinarine has been its strong DNA binding capability that were first revealed from the biophysical studies of Maiti et al., in comparison to the classical DNA intercalator ethidium.[47] These experiments were conducted above physiological pH (pH = 7.4) where both iminium and alkanolamine forms coexisted. Maiti's work has revealed that sanguinarine intercalated to DNA stronger than even ethidium, a claim recently unfounded by Hossain and Kumar from both spectral and calorimetric data.[48] It was revealed that the absorption spectrum underwent hypochromic and bathochromic effects with the exhibition of isosbestic points that indicated equilibrium between the free and the bound forms. The strong binding to DNA was also confirmed from the emission spectra of the alkaloid that was quenched in the presence of DNA. A typical absorption and fluorescence spectral titration of sanguinarine iminium with DNA is presented in Fig. 3. Further evidence for the strong binding was advanced from the thermal stabilization of the DNA against strand separation and circular dichroism changes. A typical melting profile and circular dichroism spectra of sanguinarine-DNA complexation is presented in Fig. 4. Intercalative binding was established from the viscosity studies of linear rod like DNA

and also through the unwinding rewinding mechanism of covalently closed super helical DNA.[49] A typical hydrodynamic experiment depicting the interaction is shown in Fig. 5. It was also characterized that the alkaloid which is optically inactive developed induced circular dichroism on binding to the chiral environment of the DNA.[50]

The pH dependent equilibrium between the iminium and the alkanolamine was revealed by Maiti and colleagues and it was found that the pKa was around 7.4.[51] Recent studies have suggested the pKa to be around 8.0.[32,33] The stability of the two forms was confirmed from the studies of Jones et al.[52] Subsequently, it was revealed that the iminium form is the DNA intercalator and the alkanolamine form did not exhibit any binding affinity, whatsoever, based on investigations from a number biophysical experiments.[53] A greater preponderance of the intercalating species being present at lower pH was proposed earlier by Waring from foot printing studies also.[54]

From a series of spectroscopic studies Maiti and his colleagues have evaluated the base sequence specificity and the salt dependence of the DNA binding phenomena of sanguinarine.[55-57] Sanguinarine was found to be a guanine-cytosine specific DNA intercalator from studies employing natural and synthetic DNAs. This was also confirmed by foot printing studies of Waring's group.[54] More recently using double-stranded oligodeoxynucleotides and employing spectrophotometric techniques the sequence selectivity to alternating guanine-cytosine (GC) base pairs have been

proposed.[58] The studies of Adhikari et al., have confirmed that the binding affinity was dependent on the [Na+] concentration and decreased as the [Na+] increased.[59]

Another important aspect of sanguinarine-DNA interaction is the DNA induced conversion of the alkanolamine form to the bound iminium form. Maiti and colleagues first observed that the alkanolamine form has no binding to DNA.[53] But intriguingly in the presence of high concentration of DNA there was a conversion of the alkanolamine form to the DNA bound iminium form when the experiments were performed at alkaline pH.[60,61] Typical absorption and fluorescence spectral data depicting the changes in the spectra of the sanguinarine iminium and alkanolamine form to bound iminium in the presence of DNA are shown in Fig. 6. A Schematic representation of the proposed DNA induced conversion is presented in Scheme 3. It can be observed that the spectral characteristic of the bound form is identical regardless of the pH at which the experiments were performed.

The thermodynamics of sanguinarine-DNA interaction was first reported from temperature dependent absorption spectral data by Sen and Maiti.[57] It was suggested that sanguinarine binds to natural DNAs and AT (adenine-thymine) homo and hetero polynucleotides by negative enthalpy and positive entropy changes while binding to the GC (guanine-cytosine) polynucleotides was favoured by negative enthalpy and negative entropy changes. The binding enthalpy and entropy changes were found to be strongly dependent on [Na+]. More recently the thermodynamic aspects of the interaction was studied using highly sensitive calorimetry techniques with DNA and a

number of synthetic polynucleotides.[48,59] The binding affinity of sanguinarine to natural calf thymus DNA was found to be 9.2×10^5 M^{-1} at 20 mM [Na+] and 1.21×10^6 M^{-1} at 10 mM [Na+] conditions with a stoichiometry around 2.0 base pairs, lower than the value of 3.7 at 10 mM [Na+] reported by Maiti.[57] The binding affinity was found to decrease with both increasing pH and salt concentrations. The thermodynamics of the reaction was revealed to be exothermic and enthalpy driven with significant hydrophobic contribution as observed from the heat capacity values evaluated from the variation of the enthalpy change with temperature. From detailed salt dependence study of the interaction and the parsing of the Gibbs energy changes to non-polyelectrolytic and polyelectrolytic components, it was proposed that the DNA binding of sanguinarine mostly involved non-polyelectrolytic forces although the alkaloid was positively charged. The study of Adhikari et al. also examined the thermodynamics of binding of sanguinarine to four sequences of base pairs in polynucleotides, viz. the alternating GC, alternating AT, the homo GC and homo AT sequences.[58] The comparative ITC profiles of sanguinarine binding to four sequence specific polynucleotides are presented in Fig. 7. The thermodynamic parameters of the binding to four polynucleotides are presented in Table. 2. This study unequivocally revealed the GC specificity of sanguinarine on one hand and additionally the high preference to alternating poly purine-pyrimidine sequences. Binding affinity to the alternating GC sequence was followed by alternating AT sequences. The preference to alternating purine-pyrimidine sequences was also proposed earlier from foot printing studies of Waring.[54] Recently a study on the binding

of sanguinarine to nucleosides by fluorescence quenching reported[62] of binding affinity of the order of 10^7 M^{-1}, much higher than those reported till date in a large number of studies with single and double stranded DNAs.

The first crystal structure of sanguinarine intercalated with a d(CGTACG)2 sequence was obtained by X-ray diffraction analysis at 2.3A° resolution.[63] M. Ferraroni et al. showed that the complex crystallize in the $P3_221$ space group: the asymmetric unit contains four DNA strands, arranged in a "two molecules" unit, a drug molecules, few cocrystallized water molecules, and a Ca^{+2} ion. The crystal structure of sanguinarine/ DNA complex formed by π→π interactions mainly involving the C5 and C6 residues of chain A and the G8 residues of chain D of DNA strands (Fig 8). The binding interaction is reinforced by the presence of a positive charged nitrogen atom of sanguinarine. Sanguinarine was found stacked in a non-classic intercalation site formed by six bases. X-ray results also confirmed that the iminium form to be the DNA binding moiety originally proposed by Maiti et al.[53]

Recent molecular modeling studies on the DNA binding of sanguinarine by Choi and colleagues[64] have suggested that sanguinarine intercalated into the base pairs with the isoquinoline moiety involving rings C and D (Fig. 1) as shown in Fig. 9.

6. 2. Binding to polymorphic DNA structures

Sanguinarine binding to various polymorphic DNA structures have also been investigated. Sanguinarine did not exhibit any binding to the left handed Watson-Crick base paired Z-form conformation of poly(dG-dC).poly(dG-dC) and poly(dG-

me5dC).poly(dG-me5dC); instead it cooperatively converted the Z-structure to the bound right handed B-form.[65,66] The kinetics of the B-Z transition and the effect of sanguinarine on the transitions are presented in Fig. 10. Furthermore, sanguinarine was found to convert the left handed Hoogsteen base paired H^L-form of these polynucleotides to bound right handed B-form indicating its high preference for the B-form conformation of DNA.

Spectrofluorimetric titration, electro-spray ionization time-of-flight mass spectrometry and absorbance melting methods were employed to study selectively of sanguinarine binding to bulged sites in DNA hairpins in comparison to its analogue chelerythrine.[67] The results revealed that sanguinarine binds specifically to single pyrimidine (C, T) bulge sites. The ability of sanguinarine to bind to both regular and bulged hairpins was found to be stronger than that of its analogue.

6.3. Binding to DNA triplexes

Triple helical structures are of special interest as the third strand oligonucleotide in principle can be targeted to specific genes for sequence selective recognition. But the poor stability of some of the triplexes limits their use under physiological conditions. In this context sanguinarine was explored as a specific ligand that can intercalate into triple helices and stabilize them under physiological conditions.

Lee and colleagues[68] had proposed from thermal melting studies that sanguinarine bound well to poly(dT)·poly(dA)·poly(dT) triplex (T·AxT triplex; dot and cross represent Watson-Crick and Hoogsteen base paring) and weakly to the protonated

triplex poly(C).poly(G).poly(C+) (C·GxC+ triplex). A detailed study on the binding characteristics of sanguinarine to these triplexes in comparison to the respective duplex structures was performed by Maiti and colleagues.[69] This study used optical melting, circular dichroism and temperature dependent absorption spectral analysis as probes. Typical thermal melting patterns of the sanguinarine-DNA triplex complex are presented in Fig. 11A,B. Sanguinarine was revealed to stabilize the third strand of both the DNA triplexes much stronger than their respective Watson and Crick duplexes. A comparative data on the stabilization to these triplexes and the corresponding duplexes are presented in Table 3. The binding of sanguinarine to the triplexes was further characterized by CD spectral changes with the appearance of induced CD bands in the 320-370 nm regions. It was reported that the binding to T·AxT triplex generated a negative induced CD, while with the C·GxC+ triplex the induced CD band pattern was positive in nature. Furthermore, these studies also revealed the thermodynamics of the interaction from temperature dependent absorption spectral data using van't Hoff plot. It was observed that binding of sanguinarine to T·AxT triplex was characterized by negative enthalpy and positive entropy changes, while it's binding to the C·GxC+ triplex was characterized by negative enthalpy and negative entropy changes. Overall, a stronger affinity of sanguinarine to T·AxT triplex over the C·GxC+ triplex was suggested from this study. Thus, the specificity to triplexes was to the AT sequences contrary to the GC specificity with the duplexes.

6.4. Binding to quadruplexes

Telomeric DNA and formation of G-quadruplex structures by them are considered as effective targets for anticancer therapeutic intervention. Sanguinarine being a potential anticancer agent, studies on the induction of quadruplex structures and the binding to such structures have been probed recently. Nakatani and Jiang from ESI-TOF-MS spectra, CD spectra, polymerase stop assay and melting studies reported that sanguinarine and the K+-form of G-quadruplexes dAGGG(TTAGGG)3 and dAGGG(TTAGGG)7 complexed with one sanguinarine molecule binding between G-quadruplex and two molecules of sanguinarine binding by end-stacking.[70] The ability of sanguinarine to bind and convert oligonucleotide sequence of human telomeric DNA d[5′-TTGGG(TTAGGG)3A-3′] (H24A) to specific G-quadruplex structures was investigated by Yang et al., under salt deficient conditions and reported that sanguinarine effectively converted the sequence completely to a normal anti-parallel G-quadruplex structure as inferred from the CD data.[71] It was reported that related QBAs like nitidine and chelerythrine were not so effective as sanguinarine in the case of human telomere sequence d(TTAGGG)4 [H24].[72] A subsequent study suggested that this sequence underwent a conformational transition to the Na+ form upon binding of sanguinarine in presence of K+ depending on the molar ratio of H24:SG.[73] Using spectroscopic and calorimetric techniques the binding of sanguinarine to human telomeric DNA sequence dAGGG(TTAGGG)3, has been investigated and compared with ethidium by Bhadra et al.[74] A non cooperative binding with an affinity of 10^5 M^{-1} to the quadruplex structure was observed. The binding was characterized by strong

polarization for the emission fluorescence, conformational changes, and formation of induced CD for the bound alkaloid. The typical CD spectral changes associated with the interaction are shown in Fig. 12. Calorimetric studies revealed an enthalpy and entropy favoured binding of sanguinarine to the quadruplex structure. Significant hydrophobic contribution to the binding was also proposed and enthalpy-entropy compensation behaviour was operative. The thermodynamic parameters of sanguinarine binding to quadruplex as reported to this sequence are presented in Table 4. Gosh and coworkers studied the binding of sanguinarine with two quadruplex forming sequences, human telomeric DNA (H24) and NHE III1 upstream of the P1 promoter of c-myc (Pu27) using spectroscopic techniques and suggested the association of sanguinarine to be stoichiometrically and structurally different to these sequences. They suggested that sanguinarine binds to both mixed parallel–antiparallel and all-parallel form but with higher affinity to the former.[75]

Molecular modeling studies along with CD, NMR and fluorescence of sanguinarine was performed on human telomeric G-quadruplex DNA sequences forming basket and hybrid type structures by Schwalbe and Gratteri's groups.[76] The authors used fluorescence and CD spectroscopy studies and two different modeling approaches; "an NMR driven and an unrestrained docking one". Several features of sanguinarine binding to quadruplex structures hitherto unknown were revealed. A high preference for the G-quadruplexes over duplex calf thymus DNA was not observed although higher affinity was seen from binding affinity data. This suggested the poor selectivity

of sanguinarine. The most significant features revealed, inter alia, were that the stoichiometry did not correspond to simple interaction mode involving two ligands per telomeric quadruplex, self association of the ligand induced by the quadruplex, particularly in basket type structure, and loops and groves of the quadruplex structure in basket type structure playing important role in sanguinarine binding. The docked model for sanguinarine binding to the basket type and hybrid-1 type quadruplex and the NMR driven model for the basket type G-quadruplex structure are presented in Fig 13.

Binding ability of sanguinarine to many G-quadruplex DNA sequences was evaluated by the phosphorescence recoveries of system based on L-cysteine-capped Mn-doped ZnS QDs and compared with the conformational changes probed by circular dichroism.[77] A number of studies on the binding of sanguinarine to various quadruplexes are now known.

7. 1. RNA binding properties of sanguinarine

The recent emergence of RNA as a potential drug target has fueled interest in elucidating the basics of small molecule-RNA interactions. The interaction of sanguinarine with various RNA structures has been recently investigated. Interaction of sanguinarine with A-form RNA structure of poly(I).poly(C) and poly(A).poly(U) was studied by spectroscopy and viscometry by Sen and Maiti.[78] Similar spectral manifestations as those observed with double stranded (ds) DNAs were seen with these double stranded RNAs aslo. Non co-operative binding with affinity of the order of 10^5

M^{-1} and increase in contour length of DNA were revealed. On the basis of these and other observations like stabilization against thermal strand separation and circular dichroism changes, it was concluded that sanguinarine binds to both the RNAs by a mechanism of intercalation.

The interaction of sanguinarine with the A-form and the protonated form of poly(C).poly(G) was investigated from spectroscopy, viscometry and thermodynamic studies by Das et al.[79] Thermodynamic parameters as revealed from van't Hoff plot indicated the RNA binding of the alkaloid to be an exothermic process. Sanguinarine was characterized to bind by manifesting negative enthalpy changes and positive entropy changes with both the structures. The A-form structure was suggested to be preferred over the protonated form structure by sanguinarine based on these results.

Detailed comparative structural and thermodynamic aspects of interaction to three double stranded RNAs viz. poly(A).poly(U), poly(I).poly(C) and poly(C).poly(G) was presented by Chowdhury et al.[80] This study, in contrast to the previous study of Sen and Maiti,[78] revealed co-operative binding of sanguinarine to the ds RNAs. Sanguinarine induced strong conformational changes in these RNAs. The thermodynamic of the interactions suggested that temperature dependence of the enthalpy changes afforded negative values of heat capacity changes for the binding of sanguinarine to poly(A).poly(U) and poly(I).poly(C), suggesting substantial hydrophobic contribution in the binding process. The polyelectrolytic contribution to the binding Gibbs energy in these cases was found to be less than 10%. Furthermore, an

enthalpy-entropy compensation phenomena was also suggested to occur in poly(A).poly(U) and poly(I).poly(C) systems that correlated to the strong binding involving a multiplicity of weak non-covalent interactions compared to the weak binding with poly(C).poly(G). The binding and thermodynamic parameters of sanguinarine to the ds polynucleotides are presented in Table 5.

Sanguinarine binding to the RNA triplex poly(U).poly(A)xpoly(U) was also investigated and compared with the corresponding RNA duplex, poly(U).poly(A) using a combination of spectrophotometric, thermal melting, circular dichroism techniques.[69] The interaction process was characterized by typical hypochromic and bathochromic effects in the absorption spectrum of sanguinarine, an increase of thermal melting temperature and perturbation in circular dichroism spectrum of the triplex. Scatchard analysis suggested binding to both the triplex and the duplex through non-cooperatively and the binding was stronger to triplexes than to the duplex. Sanguinarine stabilized the Hoogsteen base paired third strand as well as the Watson-Crick strands of the U.AxU triplex (Fig. 11C). Thermodynamic data from van't Hoff analysis revealed the involvement of negative enthalpy changes and positive entropy changes in the complexation. Overall, the binding of sanguinarine to the RNA triplex was much stronger than to the parent duplex.

Interaction of sanguinarine to tRNA[phe] by various biophysical and calorimetric techniques was reported by Hossain et al.[81] Co-operative binding was revealed with affinity of the order of 10^5 M^{-1}. The binding was mostly enthalpy driven and proposed

to be by an intercalation mode. From salt dependent studies the binding was inferred to involve strong non-polyelectrolytic forces. From the variation of enthalpy change with temperature the value of the heat capacity change obtained suggested the involvement of strong hydrophobic interactions in the complexation. The variation of the thermodynamic parameters of the binding is presented in Table 6. It was also observed that like in the case with single and double stranded RNAs, there was an enthalpy-entropy compensation phenomenon operating in the energetics of sanguinarine-tRNA[phe] interaction. Sanguinarine binding to single stranded RNAs other than with polyadenylic acid are not yet known but the study by Zhang et al. on nucleotides suggested that sanguinarine affinity followed the order of G > C > T > U > A at 298.15K but changed to C > G > T > U > A above 298.15 K. The binding to various nucleotides was exothermic and entropy-driven.[64]

7.2. Binding to polyadenylic acid

Due to the importance of polyadenylic acid in the post transcriptional modification of mRNA and the consequent opportunity of targeting of poly(A) tail of mRNA as a handle for therapeutic intervention, the binding of sanguinarine was investigated in details. Various spectroscopic and calorimetry techniques have been used for characterization. Sanguinarine bound to poly(A) with an affinity $(4.60 \pm 0.84) \times 10^6$ M^{-1} and it was shown that the binding to poly(A) was much preferred over many single stranded RNAs and double stranded DNAs.[82,83] The results of competition dialysis and fluorescence are shown in Fig. 14. It was found that the binding induced self-structure

in poly(A) as characterized by co-operative melting in absorbance, circular dichroism and also by a value of unity for the ratio of ($\Delta H_{cal}/\Delta H_v$) in DSC study. A typical absorption melting profile and DSC thermograms of poly(A) and poly(A)-sanguinarine complex are presented in Fig. 15. This study also characterized that sanguinarine induced self-structure due to intercalation to alternate base pairs of the self-structure. The thermodynamics of the interaction revealed favourable negative enthalpy and unfavourable entropy (negative entropy) contribution to the Gibbs energy. The binding of sanguinarine to double stranded poly(A) on the other hand was found to be two orders of magnitude lower than its affinity to single stranded poly(A). Although weak, the binding led to stabilization of the duplex structure and resulting in strong energy transfer from the adenine base pairs to the bound sanguinarine molecules that exhibited significant polarization of its fluorescence. Overall the results suggested intercalative binding that was exothermic and enthalpy driven.

8. Inhibition of sanguinarine binding by other compounds

The manifestation of the antitumor action of sanguinarine has thus been thought to derive from its strong nucleic acid binding activities. But a number of compounds may interfere with its activity by competing with it to form π-π molecular complexes, thereby blocking it from intercalating into the DNA and ultimately lowering the toxicity to the cancer cells. A typical example is the attenuation by caffeine. Although marginal, caffeine has been found to enhance the IC_{50} value of sanguinarine in cytotoxicity studies leading to its role as an "interceptor" protecting the DNA from intercalation.[84]

9. Conclusions

The nucleic acid interaction studies on the benzophenanthridine alkaloid sanguinarine spanned over 40 years now. Earlier the studies were mostly confined with DNA. More recently studies with various RNA structures have also been performed. During this period many new aspects of the interaction have been revealed. In this review, the physicochemical aspects of the data so far available in the literature have been reviewed and summarized. The studies have elucidated the mode, mechanism, affinity, base-sequence specificity, structural affinity and energetics of the interaction to both DNA and RNA. The potential of sanguinarine to bind and intercalate with high affinity to various DNA and RNA structures and induce self-structure in poly(A) is now clearly documented. A clear understanding of the sequence specificity with both double stranded DNA and RNAs, and preference to other polymorphic and higher order structures are now revealed. The structural data has been complemented by thermodynamic studies. It is expected that the complete understanding of the structural and energetics of binding along with the large biological data may help the development of sanguinarine as a potential anticancer agent in the fight of cancer.

Acknowledgements

References

1   J. Lenfeld, M. Kroutil, E. Marsálek, J. Slavík, V. Preininger and V. Simánek, *Planta Med.*, 1981, **43**, 161-165.

2   K. C. Godowski, *J. Clin. Dent.*, 1989, **1**, 96-101.

3   B. W. Obiang-Obounou, O.-H. Kang, J.-G. Choi, J.-H. Keum, S.-B. Kim, S.-H. Mun, D.-W. Shin, K. W. Kim, C.-B. Park, Y.-G. Kim, S.-H. Han and D.-Y. Kwon, *J. Toxicol. Sci.*, 2011, **36**, 277-283.

4   G. L. Southard, R. T. Boulware, D. R. Walborn, W. J. Groznik, E. E. Thorne and S. L. Yankell, *J. Am. Dent. Assoc.*, 1984, **108**, 338-341.

5   I. Slaninová, E. Táborská, H. Bochoráková and J. Slanina, *Cell Biol. Toxicol.*, 2001, **17**, 51-63.

6   V. M. Adhami, M. H. Aziz, S. R. Reagan-Shaw, M. Nihal, H. Mukhtar and N. Ahmad, *Mol. Cancer Ther.*, 2004, **3**, 933-940.

7   S. Kim, T.-J. Lee, J. Leem, K. S. Choi, J.-W. Park and T. K. Kwon, *J. Cell. Biochem.*, 2008, **104**, 895–907.

8   E. Debiton, J. C. Madelmont, J. Legault and C. Barthomeuf, *Cancer Chemother. Pharmacol.*, 2003, **51**, 474-482.

9   B.-C. Jang, J.-G. Park, D.-K. Song, W.-K. Baek, S. K. Yoo, K.-H. Jung, G.-Y. Park, T.-Y. Lee and S.-I. Suh, *Toxicol. In Vitro*, 2009, **23**, 281-287.

10 H. Ahsan, S. Reagan-Shaw, J. Breur and N. Ahmad, *Cancer Lett.*, 2007, **249**, 198-208.

11 M. H. Han, S. O. Kim, G. Y. Kim, T. K. Kwon, B. T. Choi, W. H. Lee, Y. H. Choi, *Anti-Cancer Drugs*, 2007, **18**, 913-921.

12 A. R. Hussain, N. A. Al-Jomah, A. K. Siraj, P. Manogaran, K. Al-Hussein, J. Abubaker, L. C. Platanias, K. S. Al-Kuraya and S. Uddin, *Cancer Res.*, 2007, **67**, 3888–3897.

13 M. Sun, W. Lou, J. Y. Chun, D. S. Cho, N. Nadiminty, C. P. Evans, J. Chen, J. Yue, Q. Zhou and A. C. Gao, *Genes & Cancer*, 2010, **1**, 283 –292.

14 C. Kalogris, C. Garulli, L. Pietrellaa, V.   Gambini, S. Pucciarelli, C. Lucci, M. Tilio, M. E. Zabaleta, C. Bartolacci, C. Andreani, M. Giangrossi, M. Iezzi, B. Belletti, C. Marchini and A. Amici, *Biochem. Pharmacol.*, 2014, **90**, 226-234.

15 N. Ahmad, S. Gupta, M. M. Husain, K. M. Heiskanen and H. Mukhtar, *Clin. Cancer Res.*, 2000, **6**, 1524-1528.

16 E. Seifen, R. J. Adams and R. K. Riemer, *Eur. J. Pharmacol.*, 1979, **60**, 373–377.

17 H. G. Cohen, E. E. Seifen, K. D. Straub, C. Tiefenback and F. R. Stermitz, *Biochem. Pharmacol.*, 1978, **27**, 2555-2558.

18 M. M. Chaturvedi, A. Kumar , B. G. Darnay, G. B. N. Chainy, S. Agarwal and B. B. Aggarwal, *J. Biol. Chem.*, 1997, **272**, 30129–30134.

19 M. Lopus and D. Panda, *FEBS J.*, 2006, **273**, 2139-2150.

20 V.   Simanek, R.   Vespalec, A.   Sedo, J.   Ulrichova   and   J.   Vicar, *Quaternarybenzo(c)phenanthridine alkaloids–biological activities*: *Chemical Probes in Biology*. Kluwer Academic Publishers, Netherlands, 2003, pp 245–254.

21   I. Slaninová, K. Pěnčíková, J.Urbanová, J. Slanina and E. Táborská, *Phytochem. Rev.*, 2014, **13**, 51-68.

22   J. Mallikova, A. Zdarilova and A. Hlobilkova, *Biomed. Pap. Med. Fac. Univ. Palacky. Olomouc Czech Repub.*, 2006, **150**, 5-12.

23   I. Mackraj, T. Govender and P. Gathiram, *Cardiovas. Ther.*, 2008, **26**, 75–83.

24   J.-J. Lu, J.-L. Bao, X.-P. Chen, M. Huang and Y.-T. Wang, *Evi. Based Complemen. Alternat. Med.*, 2012, Article ID 485042, 12 pages.

25   M. Maiti and G. Suresh Kumar, *J. Nucleic Acids*, 2010, Article ID 593408, 23 pages.

26   N. Samanani, D. K. Liscombe and P. J. Facchini, *Plant J.*, 2004, **40**, 302-313.

27   P. J. Facchini, *Annu. Rev. Plant Physiol. Plant Mol. Biol.*, 2001, **52**, 29-66.

28   H. H. Pauli and T. M. Kutchan, *Plant J.*, 1998, **13**, 793-801.

29   P. J. Facchini, C. Penzes, A. G. Johnson and D. Bull, *Plant Physiol.*, 1996, **112**, 1669-1777.

30   J. Psotová, B. Klejdus, R. Večeřa, P. Kosina, V. Kubáň, J. Vičar, V. Šimánek and J. Ulrichová, *J. Chromatogr. B*, 2006, **830**, 165–172.

31   M. Hanaoka, S. Yoshida, M. Annen and C. Mukai, *Chem. Lett.*, 1986, 739–742.

32   M. Janovska, M. Kubala, V. Simanek and J. Ulrichova, *Anal. Bioanal. Chem.*, 2009, **395**, 235–240.

33   M. Janovska, M. Kubala, V. Simanek and J. Ulrichova, *Phys. Chem. Chem. Phys.*, 2010, **12**, 11335–11341.

34 G. Suresh Kumar, A. Das and M. Maiti, *J. Photochem. Photobiol. A Chem.*, 1997, **111**, 51–56.

35 H. Gorner, Z. Miskolczy, M. Megyesi and L. Biczok, *Photochem. Photobiol.*, 2011, **87**, 1315–1320.

36 J. Wolff and L. Knipling, *Biochemistry*, 1993, **32**, 13334–13339.

37 M. D. Faddeeva and T. N. Beliaeva, *Tsitologiia*, 1997, **39**, 181–208.

38 B. J. R. Philogene, J. T. Arnason, G .H. N. Towers, Z. Abramowski, F. Campos, D. Champagne and D. McLachlan, *J. Chem. Ecol.*, 1984, **10**, 115-123.

39 J. T. Arnason, B. Guèrin, M. M. Kraml, B. Mehta, R. W. Redmond and J. C. Scaiano, *Photochem. Photobiol.*, 1992, **55**, 35-38.

40 M. Maiti and A. Chatterjee, *Curr. Sci.*, 1995, **68**, 734-736.

41 R. W. Tuveson, R. A. Larson, K. A. Marley, G. R. Wang and M. R. Berenbaum, *Photochem. Photobiol.*, 1989, **50**, 733-738.

42 J. Huh, A. Liepins, J. Zielonka, C. Andrekopoulos, B. Kalyanaraman and A. Sorokin, *Cancer Res.*, 2006, **66**, 3726–3736.

43 M.-C. Chang, C.-P. Chan, Y.-J. Wang, P.-H. Lee, L.-I. Chen, Y.-L. Tsai, B.-R. Lin, Y.-L. Wang and J.-H. Jeng, *Toxicol. Appl. Pharmacol.,* 2007, **218**, 143–151.

44 S. S. Matkar, L. A. Wrischnik and U. Hellmann-Blumberg, *Arch. Biochem. Biophys.*, 2008, **477**, 43–52.

45 X.-Z. Dong, M. Zhang, K. Wang, P. Liu, D.-H. Guo, X.-L. Zheng and X.-Y. Ge, *Biomed. Res. Int.*, 2013, Article ID 517698, 8 pages.

46 M. H. Han, C. Park, C.-Y. Jin, G.-Y. Kim, Y.-C. Chang, S.-K. Moon, W.-J. Kim and Y. H. Choi, *PLoS ONE*, 2013, **8**, e63425.

47 M. Maiti, R. Nandi and K Chaudhuri, *FEBS Lett.*, 1982, **142**, 280-284.

48 M. Hossain and G. Suresh Kumar, *J. Chem. Thermodyn.*, 2009, **41**, 764-774.

49 M. Maiti, R. Nandi and K. Chaudhuri, *Ind. J. Biochem. Biophys.*, 1984, **21**, 158-165.

50 M. Maiti and R. Nandi, *J. Biomol. Struct. Dyn.*, 1987, **5**, 159-175.

51 M. Maiti, R. Nandi and K. Chaudhuri, *Photochem. Photobiol.*, 1983, **38**, 245-249.

52 R. R. Jones, R. J. Harkrader and G. L. Southard, *J. Nat. Prod.*, 1986, **49**, 1109–1111.

53 A. Sen and M. Maiti, *Biochem. Pharmacol.*, 1994, **48**, 2097-2102.

54 N. P. Bajaj, M. J. McLean, M. J. Waring and E. Smekal, *J. Mol. Recognit.*, 1990, **3**, 48-54.

55 R. Nandi and M. Maiti, *Biochem. Pharmacol.*, 1985, **34**, 321-324.

56 R. Nandi, K. Chaudhuri and M. Maiti, *Photochem. Photobiol.*, 1985, **42**, 497-503.

57 A. Sen, A. Ray and M. Maiti, *Biophys. Chem.*, 1996, **59**, 155-170.

58 L.-P. Bai, Z.-Z. Zhao, Z. Cai and Z.-H. Jiang, *Bioorg. Med. Chem.*, 2006, **14**, 5439-5445.

59 A. Adhikari, M. Hossain, M. Maiti and G. Suresh Kumar, *J. Mol. Struct.*, 2008, **889**, 54-63.

60 M. Maiti, S. Das, A. Sen, A. Das, G. Suresh Kumar and R. Nandi, *J. Biomol. Struct. Dyn.*, 2002, **20**, 455-464.

61 S. Das, Biophysical studies on the interactions of benzophenanthridine alkaloids with polymorphic nucleic acid structures, PhD thesis, Jadavpur University, 2000.

62 J. Zhang, Z. Du and X. Wei, *Sci. China Chem.*, 2012, **55**, 1895–1902.

63 M. Ferraroni, C. Bazzicalupi, A. R. Bilia and P. Gratteri, *Chem. Commun.*, 2011, **47**, 4917–4919.

64 J. Li, B. Li, Y. Wu, S. Shuang, C. Dong and M. F. Choi, *Spectrochim. Acta*, 2012, **95**, 80-85.

65 S. Das, G. Suresh Kumar and M. Maiti, *Biophys. Chem.*, 1999, **76**, 199-218.

66 M. Maiti, *Ind. J. Biochem. Biophys.*, 2001, **38**, 20-26.

67 L.-P. Bai, Z. Cai, Z.-Z. Zhao, K. Nakatani and Z.-H. Jiang, *Anal. Bioanal. Chem.*, 2008, **392**, 709–716.

68 L. J. Latimer, N. Payton, G. Forsyth and J. S. Lee, *Biochem. Cell Biol.*, 1995, **73**, 11-18.

69 S. Das, G. Suresh Kumar, A. Ray and M. Maiti, *J. Biomol. Struct. Dyn.*, 2003, **20**, 703-713.

70 L.-P. Bai, M. Hagihara, Z.-H. Jiang and K. Nakatani, *ChemBioChem*, 2008, **9**, 2583–2587.

71 S. Yang, J. Xiang, Q. Yang, Q. Zhou, X. Zhang, Q. Li, Y. Tang and G. Xu, *Fitoterapia*, 2010, **81**, 1026-1032.

72 S. Yang, J. Xiang, Q. Yang, Q. Li, Q. Zhou, X. Zhang, Y. Tang and G. Xu, *Chin. J. Chem.*, 2010, **28**, 771-780.

73 S. K. Pradhan, D. Dasgupta and G. Basu, *Biochemi. Biophys. Res. Comm.*, 2011, **404**, 139–142.

74 K. Bhadra and G. Suresh Kumar, *Biochim. Biophys. Acta*, 2011, **1810**, 485–496.

75 S. Ghosh, S. K. Pradhan, A. Kar, S. Chowdhury and D. Dasgupta, *Biochim. Biophys. Acta*, 2013, **1830**, 4189–4201.

76 I. Bessi, C. Bazzicalupi, C. Richter, H. R. A. Jonker, K. Saxena, C. Sissi, M. Chioccioli, S. Bianco, A. R. Bilia, H. Schwalbe and P. Gratteri, *ACS Chem. Biol.*, 2012, **7**, 1109–1119.

77 L.-N. Wen and M.-X. Xie, *J. Photochem. Photobiol. A Chem.*, 2014, **279**, 24–31.

78 A. Sen and M. Maiti, *Ind. J. Biochem. Biophys.*, 2002, **39**, 106-112.

79 S. Das, A. Banerjee, A. Sen and M. Maiti, *Curr. Sci.*, 2000, **79**, 82-87.

80 S. Roy Chowdhury, M. M. Islam and G. Suresh Kumar, *Mol. BioSyst.*, 2010, **6**, 1265–1276.

81 M. Hossain, A. Kabir and G. Suresh Kumar, *J. Biomol. Struct. Dyn.*, 2012, **30**, 223-234.

82 P. Giri and G. Suresh Kumar, *Biochim. Biophys. Acta*, 2007, **1770**, 1419–1426.

83 P. Giri and G. Suresh Kumar, *J. Photochem. Photobiol. A Chem.*, 2008, **194**, 111–121.

84 G. M. Hill, D. M. Moriarity and W. N. Setzer, *Sci. Pharma.*, 2011, **49**, 729-747.

Table 1: Physiochemical properties of sanguinarine

Emperical formula	$C_{20}H_{14}O_4N^+$
Chemical name	13-Methyl-[1,3]-benzodioxolo[5,6-*c*]-1,3-dioxolo[4,5-*i*]phenanthridin-13-ium
Molecular weight (ion)	332.33
polar surface area	40.8 Å^2
Crystal colour	orange-red
Solubility	water: slightly soluble <0.3 mg/mL
Melting point (ºC)	278 - 279 °C
Optical rotation [α]$_D$ (solvent)	0ºC (H$_2$O)
Peak position of absorption spectrum (nm)	273, 327, 400, and 470 nm (in aqueous buffer of pH 6.0)
Molar extinction coefficient (ε) (M^{-1} cm^{-1})	30,700 at 327 nm
Peak position of fluorescence spectrum (nm)	Strong, at 570 nm
pKa	8.06
IC$_{50}$ or LD$_{50}$ value (in mice)	19.4 mg/kg of body-weight

Table 2: ITC derived thermodynamic parameters for the binding of sanguinarine to various polynucleotides in citrate phosphate buffer of 20 mM [Na+], pH 5.2 at 20°C (Ref. 59)

Polymer	K_b (x10^6 M^{-1})	N	ΔH^O(kcal mol^{-1})	$T\Delta S^O$(kcal mol^{-1})	ΔG^O(kcal mol^{-1})
poly(dG-dC).poly(dG-dC)	6.03	0.47	-9.04	0.58	-9.62
poly(dA-dT).poly(dA-dT)	3.01	0.48	-7.16	1.53	-8.69
poly(dG).poly(dC)	0.46	0.40	-4.37	3.19	-7.56
poly(dA).poly(dT)	1.31	0.21	5.76	13.94	-8.18

Table 3: Effect of sanguinarine on the thermal stability of triplexes and duplexes [a] (Ref. 61)

Polymer/Complex	D/P	[Na$^+$] (mM)	Tm′ (°C) 3 →2	Tm″ (°C) 2 →1	ΔTm′ (°C) 3 →2	ΔTm″ (°C) 2 →1
T.AxT	0	310	55.1	75.6		
T.AxT + SG	0.01	310	57.3	76.5	2.2	0.9
	0.025	310	64.4	77.4	9.3	1.8
	0.10	310	77.8	77.8	22.7	2.2
	0.20	310	79.6	79.6	24.5	4.0
A.T[b]	0	310		76.5		
A.T + SG	0.10	310		79.1		2.6
	0.20	310		81.0		4.5
C.GxC$^+$	0	60	59.0	88.5		
C.GxC$^+$ + SG	0.06	60	64.5	91.3	5.5	2.5
	0.10	60	66.5	92.5	7.5	4.0
G.C[b]	0	60		87.9		
G.C + SG	0.058	60		90.4		2.5
	0.098	60		92.2		4.3
U.AxU	0	35	36.0	45.5		
U.AxU + SG	0.02	35	40.0	50.0	4.0	4.5
	0.05	35	45.5	54.0	9.5	8.5
	0.10	35	48.0	55.2	12.0	9.7
	0.20	35	51.1	57.0	15.1	11.5
A.U[b]	0	35		45.5		
A.U + SG	0.05	35		52.7		7.2
	0.10	35		54.5		9.0
	0.20	35		57.5		12.0

[a] Average from three experiments. Error limits for individual measurements are estimated at ±0.5°C in Tm. Tm′ (3 →2) and Tm″ (2→1) are triplex to duplex and duplex to single stranded transition, respectively. ΔTm = [Tm of complex–Tm of triplex or duplex]. [b] Only single Tm was observed in this case.

Table 4: Thermodynamic parameters for the binding of sanguinarine to the quadruplex DNA (Ref. 74)

Temperature (K)	Kb (x10^6 M^{-1})	ΔH^O (kcal mol^{-1})	$T\Delta S^O$ (kcal mol^{-1})	ΔG^O (kcal mol^{-1})	ΔCp^O (kcal mol^{-1}K^{-1})	ΔG_{hyd}^O (kcal mol^{-1})
283.15	11.1 ± 0.07	−3.25	5.93	−9.18	−0.198	−15.8
288.15	7.82 ± 0.08	−4.10	5.04	−9.14		
298.15	2.41 ± 0.02	−6.00	2.70	−8.75		
303 .15	0.90 ± 0.03	−7.05	1.25	−8.30		

All the data in this table are derived from ITC experiments conducted in MOPS buffer, pH 6.81. Kb and ΔH^O and $T\Delta S^O$ values were determined from ITC profiles fitting to Origin 7 software. The values of ΔG^O and ΔG_{hyd}^O were determined using the standard equations $T\Delta S^O = \Delta H^O - \Delta G^O$ and $\Delta G_{hyd}^O = 80$ (±10) × ΔCp^O.

Table 5: Temperature dependent thermodynamic parameters for the association of sanguinarine with the three ds RNAs (Ref. 80)

RNAs	Temp. (K)	K_b (x10^5 M^-1)	ΔH^O (kcal mol^-1)	$T\Delta S^O$ (kcal mol^-1)	ΔG^O (kcal mol^-1)	ΔCp^O (cal mol^-1 K^-1)	ΔG_{hyd}^O (kcal mol^-1)
poly(A).poly(U)	283.15	10.4	-5.91	1.89	-7.80	-135	-10.8
	293 .15	9.22	-7.09	0.91	-8.00		
	303.15	8.96	-8.61	−0.35	-8.26		
Poly(I).poly(C)	283.15	10.0	-2.63	5.55	-8.18	-134	-10.7
	293 .15	8.67	-4.34	3.56	-7.90		
	30.3.15	5.85	-5.61	2.39	-8.00		
Poly(C).poly(G)	283.15	5.45	-3.84	3.59	-7.43	-28	-2.2
	293 .15	3.47	-4.19	3.29	-7.43		
	30.3.15	0.35	-4.39	1.91	-6.30		

All the data in this table are derived from ITC experiments in cacodylate buffer of 20 mM [Na+], pH 6.5.

Table 6: ITC derived thermodynamic parameters for the binding of sanguinarine to tRNA[Phe] in citrate phosphate buffer of 2 mM [Na+], pH 6.25 at different temperatures (Ref. 81)

Temperature (K)	K_b (x10^{5}M^{-1})	N	ΔH^O (kcal mol^{-1})	$T\Delta S^O$ (kcal mol^{-1})	ΔG^O (kcal mol^{-1})	ΔCp^O (cal mol^{-1}K^{-1})
283.15	13.80 ± 0.95	0.159 ± 0.002	−3.78 ± 0.04	4.160	−7.94 ± 0.04	−184.5 ± 8.4
288.15	10.30 ± 0.67	0.162 ± 0.002	−4.52 ± 0.05	3.398	−7.92 ± 0.05	
293 .15	8.15 ± 0.49	0.164 ± 0.002	−5.52 ± 0.05	2.409	−7.93 ± 0.05	
398 .15	5.50 ± 0.36	0.183 ± 0.004	−6.53 ± 0.68	1.305	−7.83 ± 0.68	
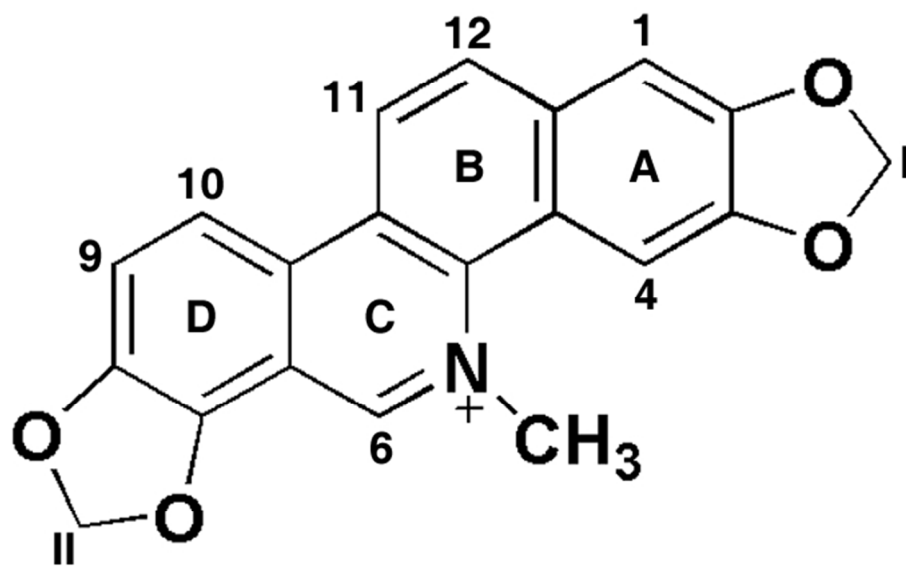
Fig. 1 Molecular structure of sanguinarine.
63x40mm (300 x 300 DPI)
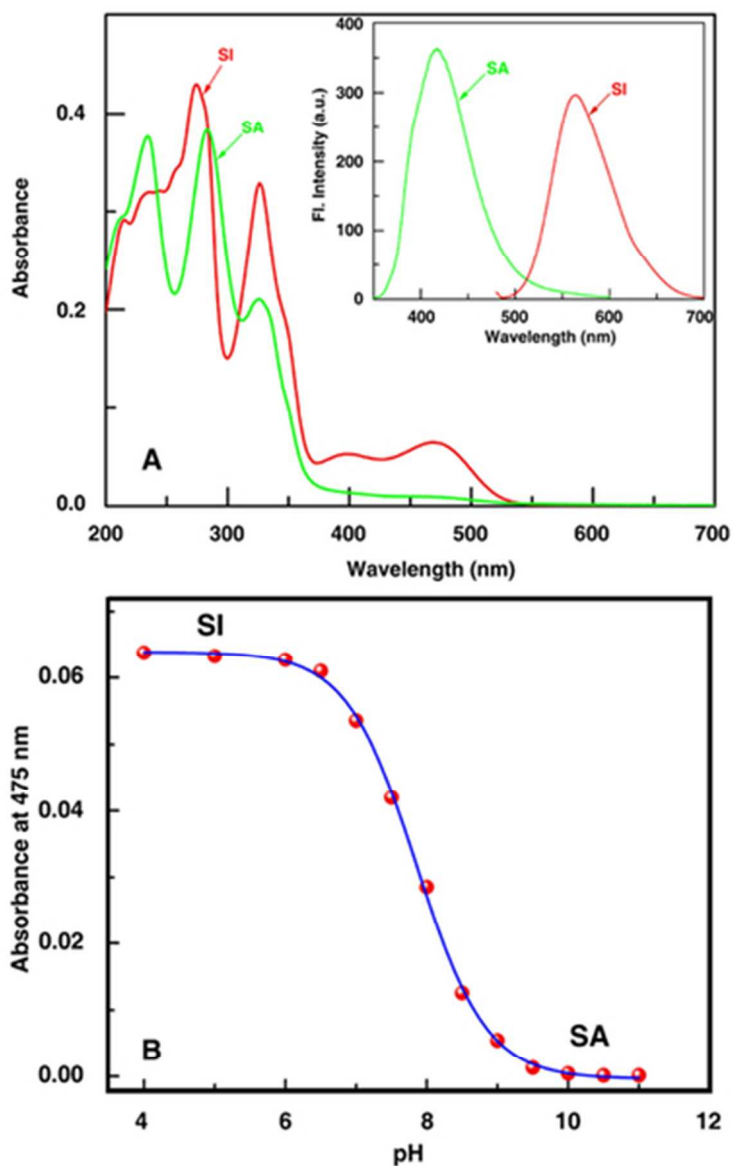
Fig. 2 Panel A: Characteristics absorption spectra of sanguinarine iminium (SI) and alkanolamine (SA) forms. Inset shows the fluorescence emission spectra of iminium and alkanolamine forms of sanguinarine. Panel B: pH titration of sanguinarine in aqueous buffer of various pH in the 4 to 11 ranges obtained from spectrophotometric measurements at 475 nm.
33x52mm (300 x 300 DPI)
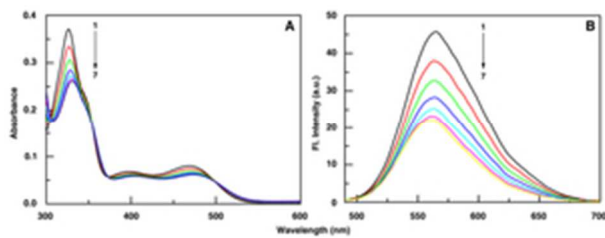
Fig. 3 (A) Absorption spectral changes of SI (10 µM, curves 1-7) treated with CT DNA with P/D 0, 1, 2, 4, 6, 8, and 12. (B) Fluorescence spectral changes of SI (2.5 µM, curves 1–7) in presence with 0, 2.5, 7.5, 15, 25, 30, 40 µM of CT DNA.
25x9mm (300 x 300 DPI)
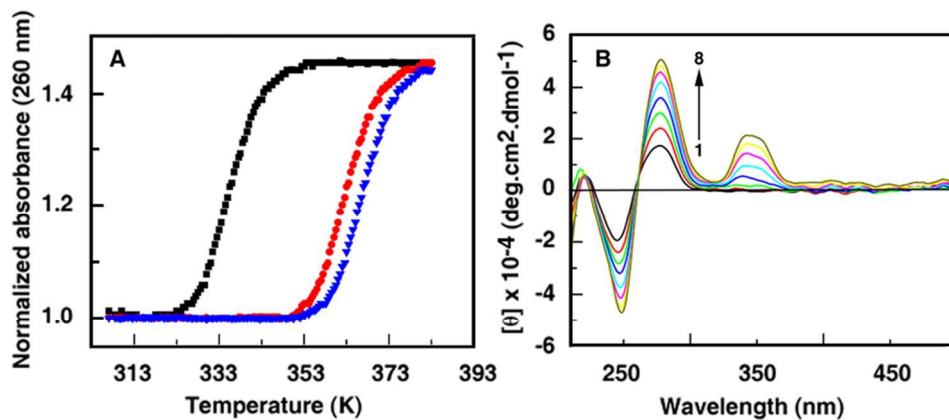
Fig. 4 Panel A: Plot of relative absorbance against temperature to show the thermal melting profiles of CT DNA (20 μM) (■) treated with 16 (•), 20 μM (▲) of sanguinarine. Panel B: Change in circular dichroic spectra of CT DNA (30 μM, curves 1–8) treated with 0, 1.5, 3.0, 4.5, 6.0, 7.5, 9.0 and 10.5 μM of sanguinarine at 100 mM [Na+]. Reproduced from Ref. 48 with permission. Copyright 2008 Elsevier Ltd.
352x149mm (72 x 72 DPI)
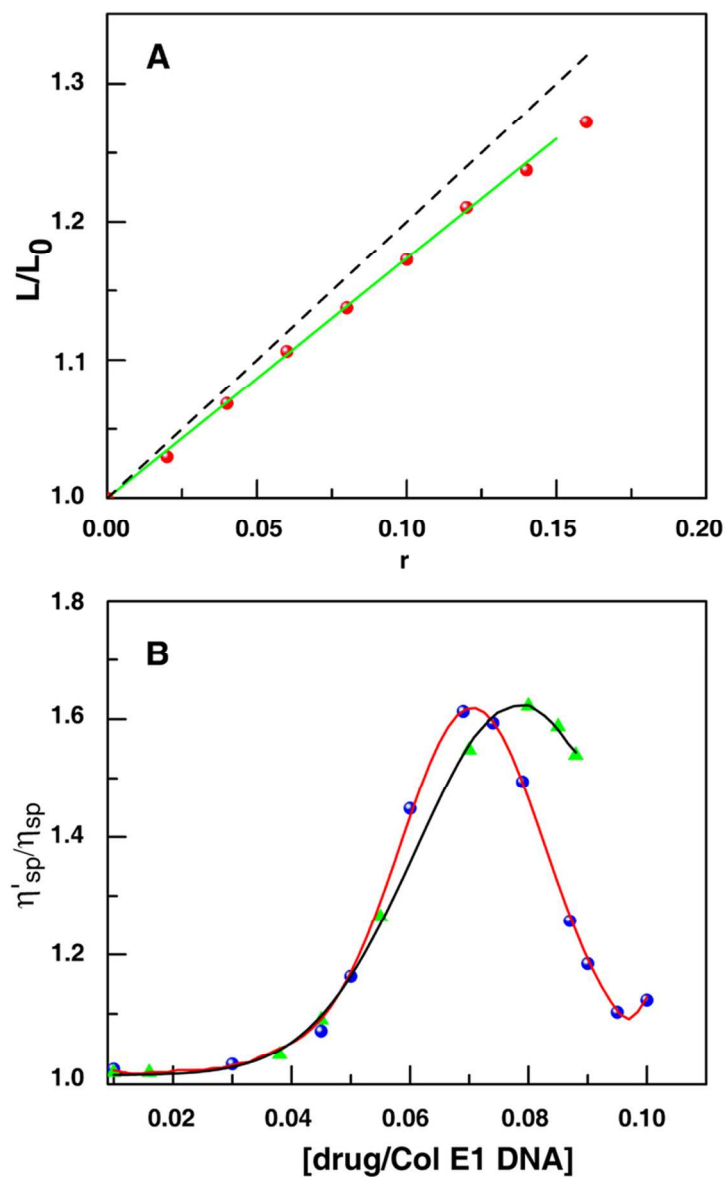
Fig. 5 Panel A: Influence of SG on the relative contour length of sheared rod-like CT DNA. Panel B: Viscometric titration of CCS Col E1 DNA by SG (•--•) and ethidium bromide, (∆--∆) in 0.015 M NaCl + 0.0015 M trisodium citrate (pH = 7.1) [Viscocity expressed by the specific viscosity of sanguinarine bound Col E1 DNA solution relative to that of respective Col E1 DNA solution alone was plotted with increasing drug to DNA concentration which represents the increasing value of r for each drug. Reproduced with permission from Ref. 49.
67x108mm (300 x 300 DPI)
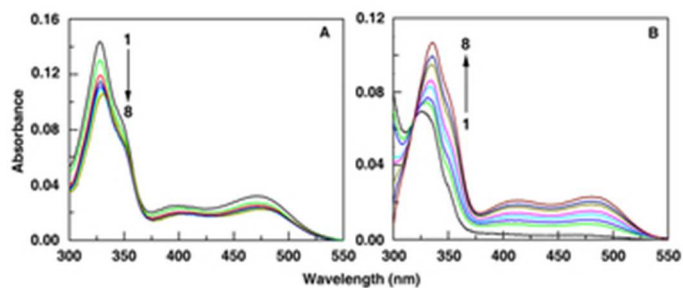
Fig. 6 (A) Absorption spectra of sanguinarine iminium form (5 µM) treated with 0, 2, 4, 6, 10, 20, 30 and 40 µM (curves 1–8) of CT DNA in 20 mM citrate phosphate buffer, pH 5.2. (B) Absorption spectra of sanguinarine alkanolamine form (5 µM) treated with 0, 300, 400, 500, 600, 800, 900 and 1000 µM (curves 1–8) of CT DNA in 20 mM [Na+] carbonate bicarbonate buffer, pH 10.4.
28x12mm (300 x 300 DPI)
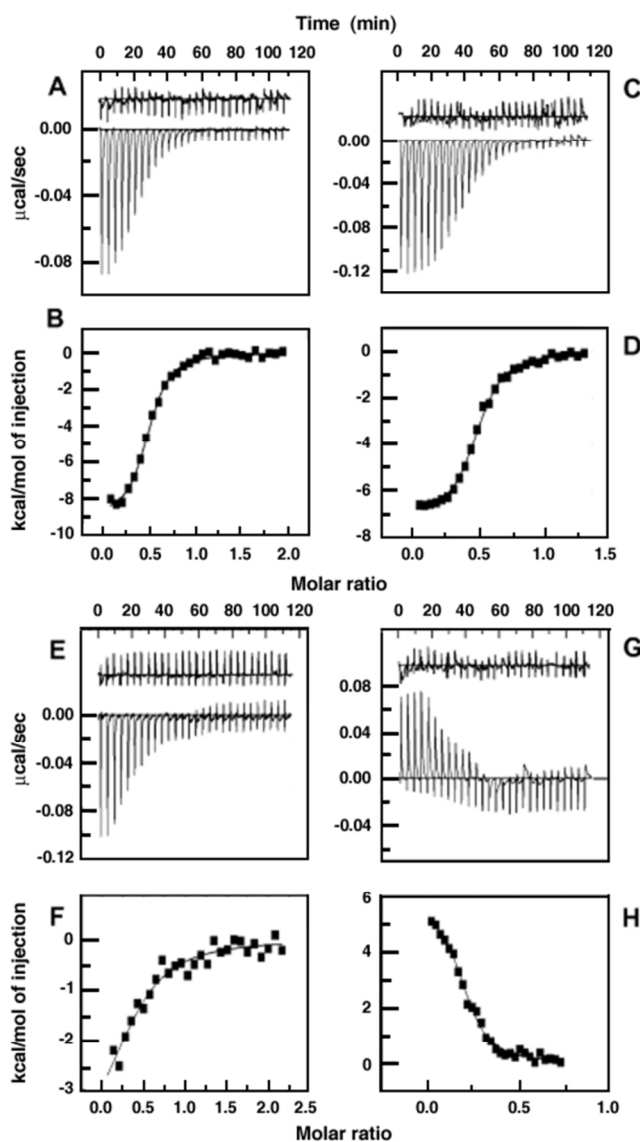
Fig. 7 ITC profiles for the binding of sanguinarine to poly(dG-dC).poly(dG-dC) (A and B), poly(dA-dT).poly(dA-dT) (C and D), poly(dG).poly(dC) (E and F) and poly(dA).poly(dT) (G and H) in CP buffer, 20 mM [Na+], pH 5.2 at 20 oC. Reprinted from Ref. 59 with permission. Copyright 2008 Elsevier B. V. 31x53mm (600 x 600 DPI)
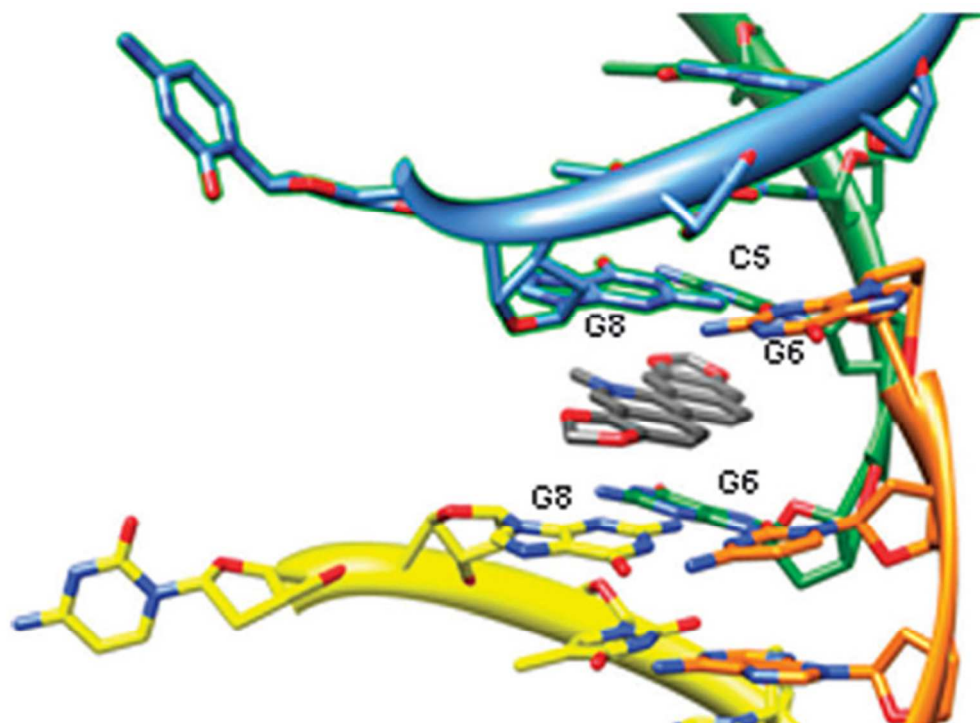
Fig. 8 Sanguinarine molecule intercalated at the interface of two "two molecules" DNA units. DNA chains color scheme: A = orange, B = yellow, C = green, D =blue. Reprinted from Ref. 63 with permission. Copyright The Royal Society of Chemistry 2011.
305x223mm (72 x 72 DPI)
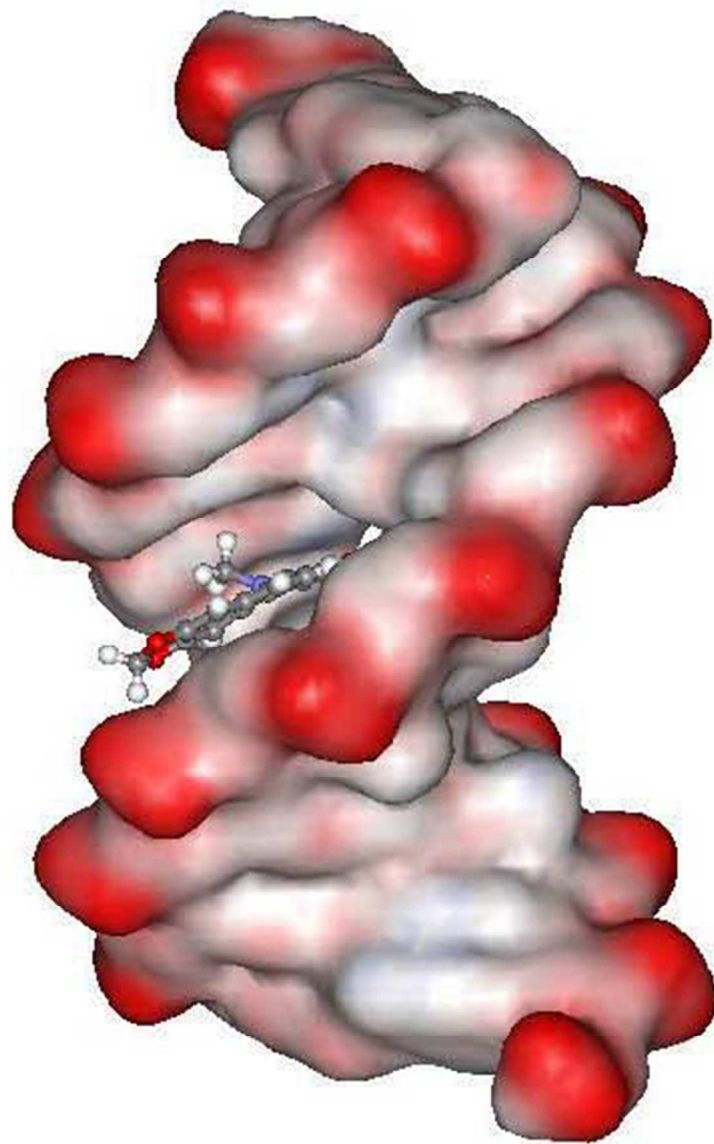
Fig. 9 Molecular model for the interaction of sanguinarine with DNA. Reprinted from Ref. 64 with permission. Copyright 2012 Elsevier B.V.
99x153mm (96 x 96 DPI)
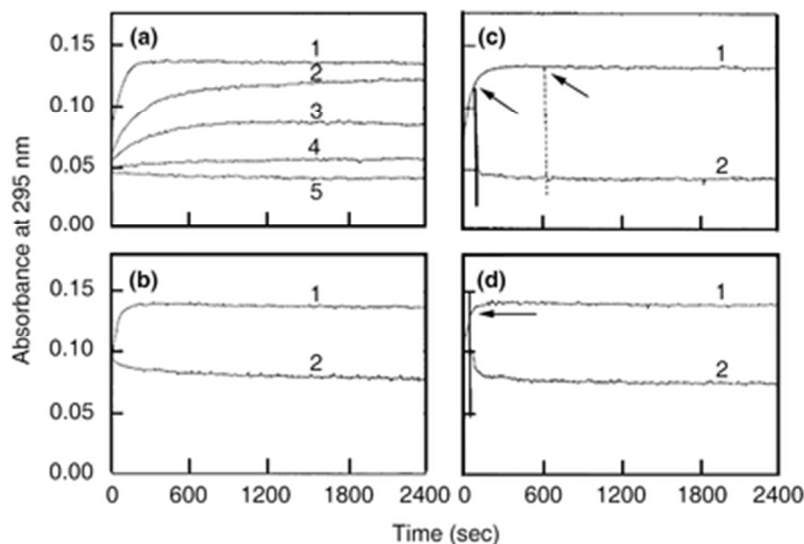
Fig. 10 Kinetic analysis of B to Z transition of 49.0 μM of poly[d(G-C)] and 51.0 μM poly[d(G-me5C)] in absence and presence of different amounts of sanguinarine. The reaction was initiated by adding polynucleotide to the buffer containing different amounts of sanguinarine as represented in (a) by curves 1 (0 μM), 2 (2.45 μM), 3 (4.90 μM), 4 (9.80 μM) and 5 (14.70 μM) and (b) by curves 1 (0 μM) and 2 (15.30 μM). Reversal of the B to Z transition by sanguinarine is presented in (c) and (d) for poly[d(G-C)] and poly[d(G-me5C)], respectively. The transition was initiated as described above but was interrupted by adding sanguinarine at the points indicated by the arrows. (c) and (d) represent the change in absorbance in the absence (curve 1) and in the presence (curve 2) of 14.7 μM and 15.30 μM sanguinarine, respectively. Reprinted from Ref. 65 with permission. Copyright 1999 Elsevier Science B. V.
17x11mm (600 x 600 DPI)
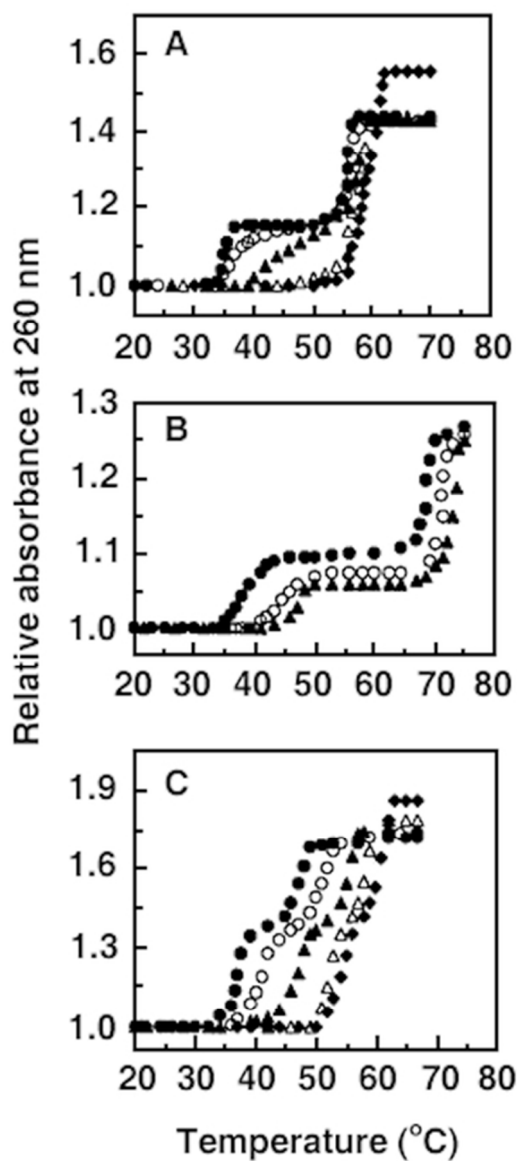
Fig. 11 Thermal melting profiles of DNA and RNA triplexes and their complexation with sanguinarine. (A) 20.0 μM of T•AxT triplex (•) and its complexation with sanguinarine at D/P of 0.01 (○), 0.025 (▲), 0.1 (Δ) and 0.2 (•) in SCH buffer I; (B) 40.12 μM of C•GxC+ triplex (•) and its complexation with sanguinarine at D/P of 0.06 (○) and 0.1 (▲) in SCH buffer III; (C) 28.0 μM of U•AxU triplex (•) and its complexation with sanguinarine at D/P of 0.05 (○), 0.1 (▲-▲), 0.2 (Δ-Δ) and 0.3 (•) in SCH buffer IV. Reproduced with permission from Ref. 61.
17x35mm (600 x 600 DPI)
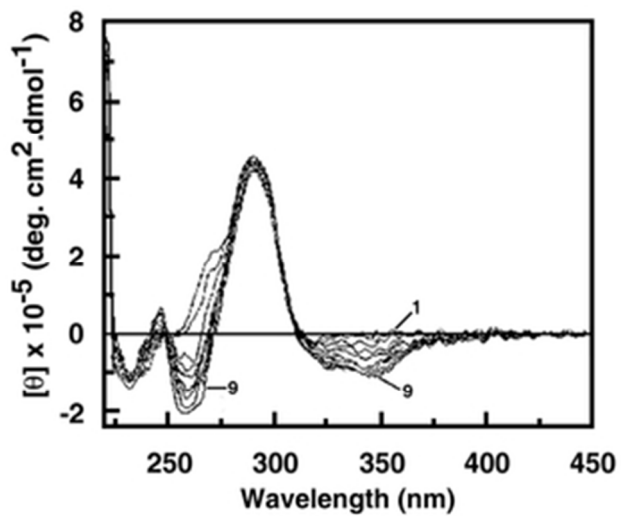
Fig. 12 Representative CD spectra resulting from the interaction of quadruplex DNA (6 μM) in the absence (spectrum 1) and presence of successive additions of sanguinarine in 50 mM MOPS buffer containing 0.1 M KCl, pH 6.81, at 25 °C. The expressed molar ellipticity is based on the oligonucleotide concentration. Reproduced with permission from Ref. 74. Copyright 2011 Elsevier B. V.
13x10mm (600 x 600 DPI)
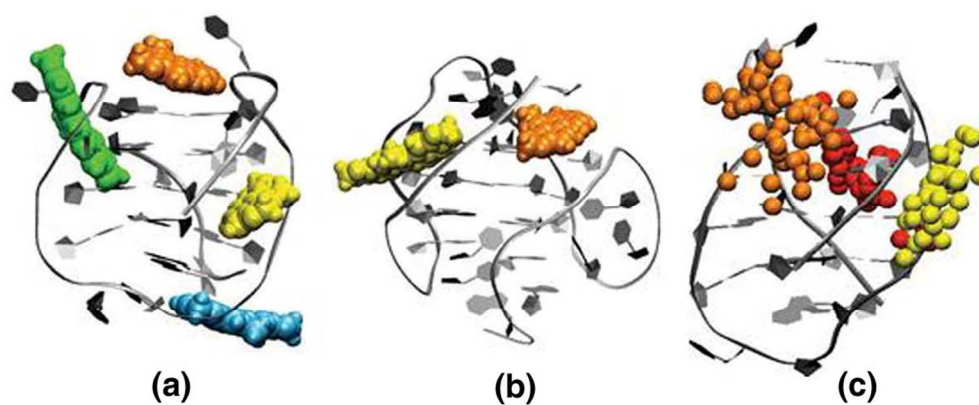
Fig. 13 Unsaturated-docking poses within 15kcal/mol from the lowest in energy, obtained for the adducts between (a) sanguinarine and basket-type G-quadruplex DNA and (b) sanguinarine and hybrid-1 type DNA. Overlay of the 50 low-energy representative NMR-driven docking models obtained for the Tel22: SG complex. The ligands are represented as their centroid. Reproduced with permission from Ref. 76. Copyright 2012 American Chemical Society.
320x133mm (96 x 96 DPI)
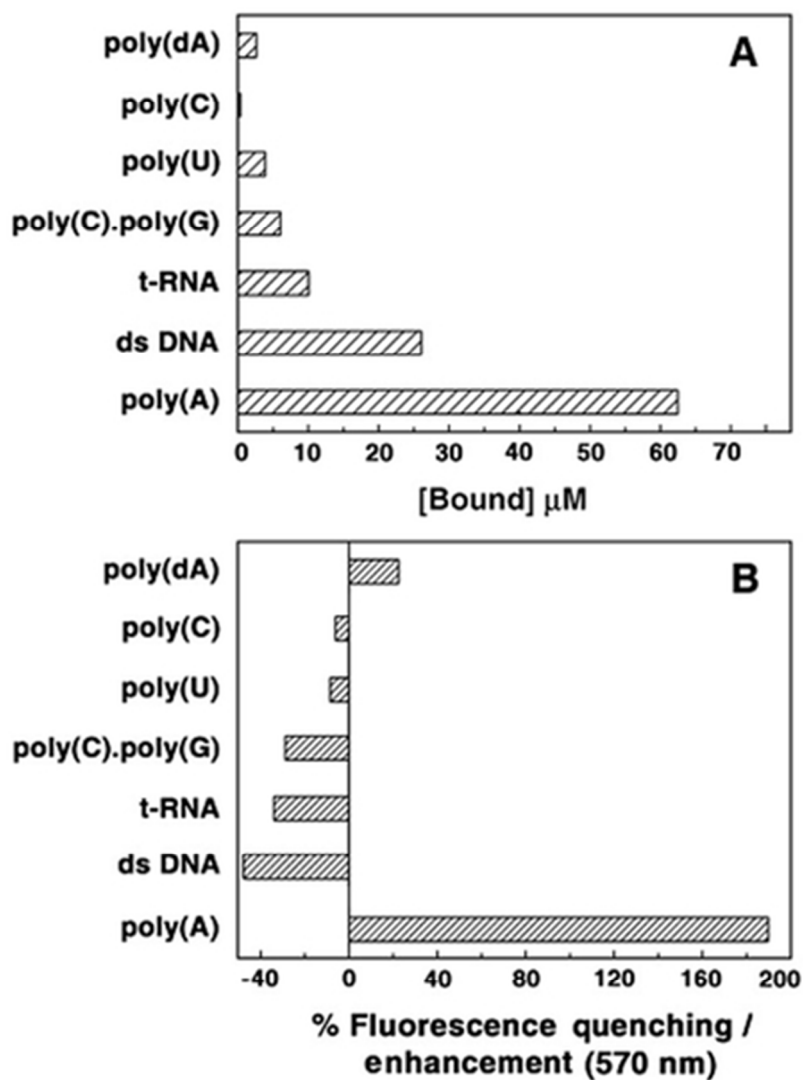
Fig. 14 Top panel: result of competition dialysis experiment showing preferential binding of sanguinarine to poly(A). Bottom panel: relative steady state fluorescence intensity of sanguinarine (2.42 µM) at 570 nm in presence of various polynucleotides at polynucleotide monomeric unit/drug molar ratio (P/D) 12. These experiments were performed in Citrate-Phosphate buffer, pH 6.5 at 20 ± 0.5 °C. Reprinted from Ref. 82 permission. Copyright 2007 Elsevier B.V.
34x47mm (300 x 300 DPI)
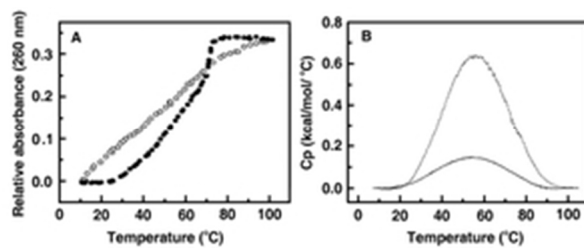
Fig. 15 Panel A: UV melting profile of poly(A) (100 µM) (○) and poly(A)–SG complex (D/P = 0.25) (●) monitored at 260 nm. Panel B: DSC thermograms of 1 mM of poly(A) (solid curve) and complex of 1 mM of poly (A) and 250 µM of sanguinarine (dashed curve). Reproduced from Ref. 82 with permission. Copyright 2007 Elsevier B.V.
12x5mm (600 x 600 DPI)
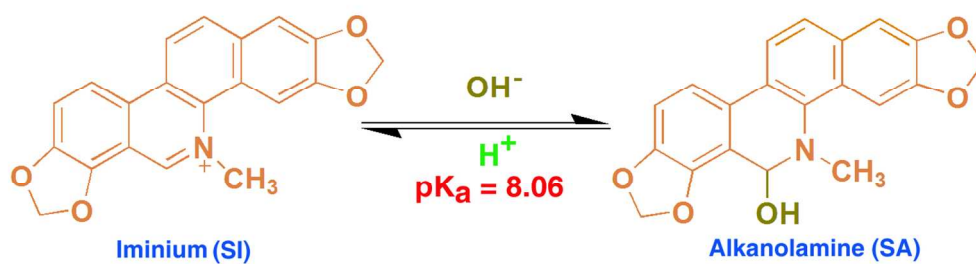
Scheme 1 pH dependent chemical structure change of sanguinarine iminium (SI) and alkanolamine (SA) forms.
117x33mm (300 x 300 DPI)
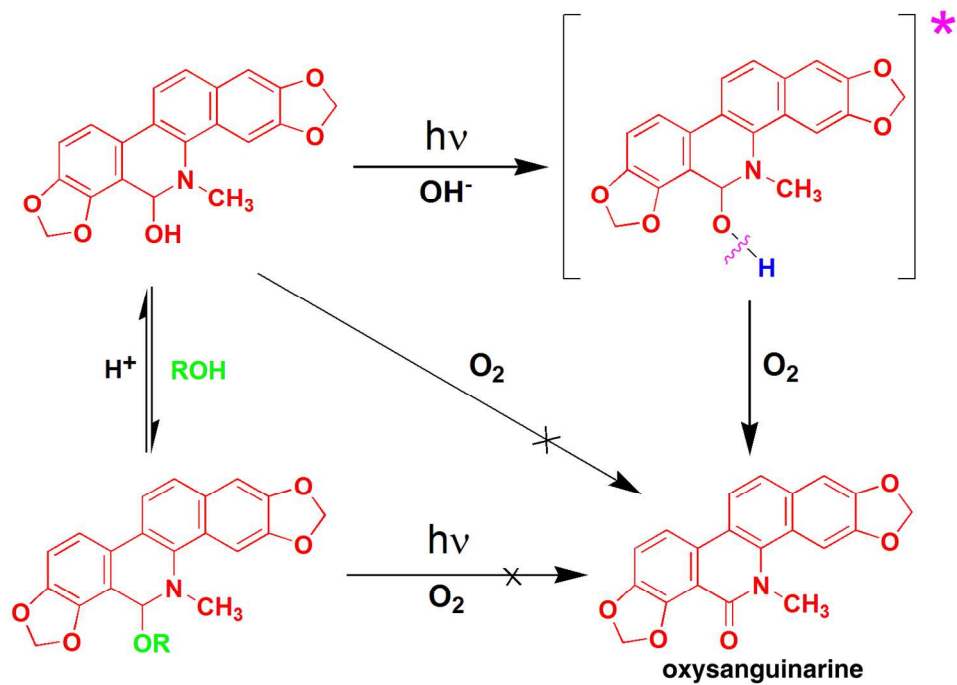
Scheme 2 Generation of oxysanguianrine from sanguinarine alkanolamine in presence of oxygen by photochemical process. Reprinted from Ref. 34 with permission. Copyright Elsevier Science S. A. 139x95mm (300 x 300 DPI)
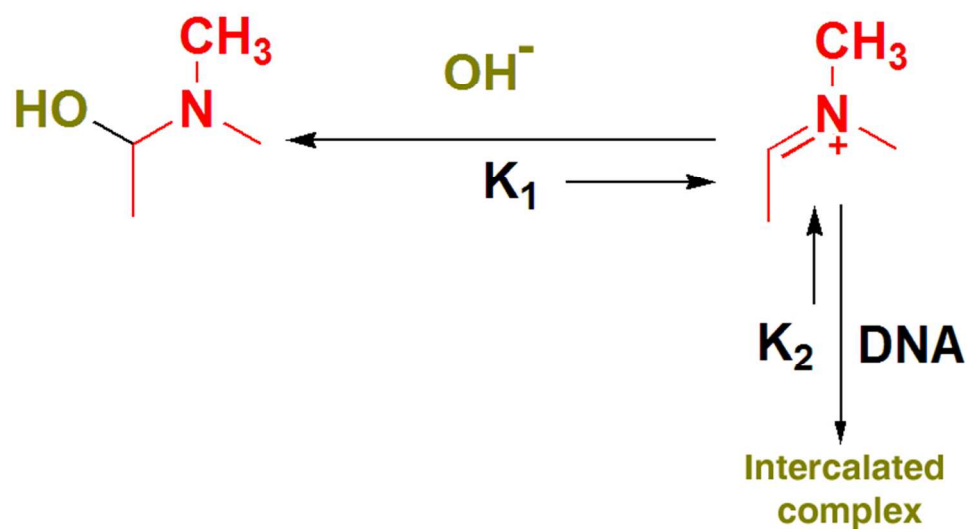
Scheme 3 A Schematic representation of the DNA induced conversion alkanolamine to bound iminium.
Reprinted from Ref. 61 with permission.
69x38mm (300 x 300 DPI)

Author Biography

G. Suresh Kumar

Dr. G. Suresh Kumar, Senior Principal Scientist at the CSIR-Indian Institute of Chemical Biology, Kolkata, did his PhD in Chemistry from the University of Delhi. He studied the interaction of natural alkaloids with polymorphic nucleic acid structures. He was a visiting scientist at the City University of New York, Hunter College, New York, USA during 1993-1995 and 1999-2001 and studied the covalent alkylation of DNA by the anticancer agent mitomycin C. He is the author of more than 155 original peer reviewed publications. His research interests are Nucleic acid and protein structure, and chemical biology of drug-nucleic acid/protein interactions.

Soumitra Hazra

Soumitra Hazra received his Bachelor of Science (B.Sc.) with Chemistry honors from Vidyasagar University, West Bengal, India in 2008. Then he moved to Indian Institute of Technology Madras (IITM), Chennai, India to pursue Master of Science in Chemistry. Present, he is a Ph.D. student as CSIR-senior research fellow in the Biophysical Chemistry Laboratory of Indian Institute of Chemical Biology, Kolkata, India. His current research interest includes studies on the interaction of therapeutically important alkaloids and analogues with biomolecules like protein and nucleic acids, micelle driven 'de-intercalation' of drugs and mutagens, and understanding the inclusion phenomena with supramolecular host.